

Study of EMI-Based Damage Type Identification in a Cracked Metallic Specimen Repaired by a Composite Patch*

Amir Hossein Keshvari Fard[□] ¹, Roohallah Ghasemi², Bijan Mohammadi³

¹*School of Aerospace Engineering, Sharif University of Technology, Tehran, Iran*

²*School of Mechanical Engineering, Tehran University, Tehran, Iran*

³*School of Mechanical Engineering, Iran University of Science and Technology, Tehran, Iran*

Abstract: Using adhesively bonded composite patch repairs has been increased in various industries to improve the structural integrity of cracked metallic structures in recent decades. Monitoring of crack propagation and composite patch debonding, as two dominant failure mechanisms in this repair technique, plays a significant role in the integrity assessment of the component. This research conducts an experimental investigation on the simultaneous monitoring of these two failure mechanisms in a cracked metallic specimen repaired by a composite patch. For this purpose, the electromechanical impedance method was used to evaluate the feasibility of recognizing the type of damage at any phase of total damage propagation process. Two piezoelectric sensors were implemented, one mounted on the metal and the other on the composite patch. Investigation of impedance spectrums and damage index trends showed that debonding and crack propagation produce different effects on the measurements made by sensors. These differences were used as a basis of identifying the type of damage. As a result, some features were introduced to classify the type of damage in each step of damage propagation.

Keywords: Crack, Debonding, Electromechanical Impedance, Piezoelectric, Structural Health Monitoring, Composite Patch, Damage Index

* This is a preprint of the Work accepted for publication in *Russian Journal of Nondestructive Testing*, ©, copyright 2019, Springer

[□] Corresponding author. E-mail: akeshvari@alum.sharif.edu

1 Introduction

During recent decades, composite patches have been widely used to repair cracked and corroded metallic components in various industries [1]. This method is an efficient approach to extend the life of structures as well as maintaining their efficiency [2]. Adhesively bonded composite patches have many advantages such as improving fatigue behavior, maintaining strength and stiffness, reducing corrosion effects, and easy implementation on complex surfaces [1]. However, the two significant sources of damage in this kind of repair are debonding of the patch from the structure and propagation of cracks in the damaged structure under the patch. Obtaining information about the state of crack propagation and debonding is the most critical factor in determining the health of repair and its efficiency. Since the damage of metallic components is not visible after the repairing process, it is a challenging task to acquire a proper perception about the repair efficiency in critical parts of a structure, particularly on inaccessible components and where conducting non-destructive tests are not easily feasible.

To solve this problem, it seems necessary to use structural health monitoring (SHM) technologies to evaluate the condition of these repairs continuously, especially at those critical points of structure which are not readily accessible. Generally, a structural health monitoring system is a combination of sensors (and possibly actuators and processors) embedded in a structure, which should determine the presence of a defect, defect location, defect size, residual strength, structural reliability, and integrity at any moment [3]–[5]. Structural health monitoring system causes the inspections to be implemented according to structural conditions and not after a certain number of service hours. As a result, this approach leads to reduced maintenance cost by changing the maintenance strategy from scheduled-based maintenance to condition-based maintenance.

One of the significant challenges in repaired structures is identifying the most probable location where damage propagation occurs. An adhesively bonded composite patch repaired component is considered as a critical hot spot that is susceptible to crack propagation and debonding failure mechanisms. If the location of the damage is specified, there will be no need to identify the damage location. Hence, employing local techniques for structural health monitoring is more convenient.

Among the various SHM techniques, the electromechanical impedance (EMI) method is an effective local method due to its high precision, low cost, and easy implementation. This technique is classified as a vibration-based method and uses piezoelectric sensors to determine the structural condition [6]. Because of the performance of piezoelectric sensors at high frequencies [7], these

sensors are particularly useful for detecting damages in the early steps of their formation, which cannot be detected by traditional vibration-based techniques [8]. Other advantages of the EMI method include further ease of use in complex structures, less expensive equipment, and simple data acquisition. Since the output data in this method is in the frequency domain, its processing and interpretation need less effort. Also, due to local excitation and measurement in the EMI method, the damage detection process is not affected by boundary conditions or ambient vibrations. Therefore, this method is very efficient for detecting local damages, and in some cases, it is also an ideal health monitoring solution where the potential damage locations are known, such as repaired components [9].

The EMI method is based on the principle that any damage propagation affects structural stiffness and damping properties of a structure. Changing these properties causes changes in the mechanical impedance of the structure. Since the direct measurement of the mechanical impedance of a component is a complicated process, the electromechanical coupling of piezoelectric materials is utilized to estimate the mechanical impedance. In other words, any damage and subsequent changes of the mechanical impedance can be detected through observing the variations of the piezoceramic electrical impedance, which is located in the vicinity of the damage [8]. For example, structural damage changes the natural frequency of the system and displaces the peaks, introducing new peaks and valleys in the impedance spectrum measured by the sensor [10].

Figure 1 shows a simple electromechanical model schematically. In this model, a piezoelectric sensor is connected to a single-degree-of-freedom system consisting of a mass, a spring, and a damper. According to Equation 1, the electrical admittance of the sensor, $Y(\omega)$ (the reciprocal of electrical impedance), is a function of the mechanical impedance of the piezoelectric sensor, $Z_a(\omega)$, and mechanical impedance of Structure, $Z_{str}(\omega)$.

$$Y(\omega) = Z^{-1}(\omega) = i\omega C \left(1 - \kappa_{31}^2 \frac{Z_{str}(\omega)}{Z_{str}(\omega) + Z_a(\omega)} \right) \quad (1)$$

Where C is the electric capacity, and κ_{31}^2 is the piezoelectric coupling constant. All the parameters except the mechanical impedance of the main structure $Z_{str}(\omega)$ result from the piezoelectric properties. Therefore, the only determinant variable for the electrical impedance of the sensor is the mechanical impedance of the structure, and the electrical impedance is affected by the variations in the mechanical impedance of the structure. Consequently, the existence of any damage can be detected by comparing the electrical impedance spectrum of a damaged structure and the spectrum under the pristine condition as a baseline [8].

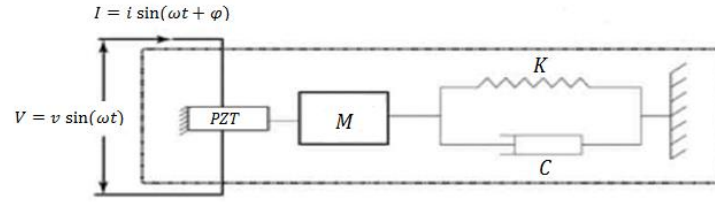


Figure 1. Schematic of an electromechanical model [8]

The EMI-based SHM method also uses damage indices to detect the existence of damage [11]–[15]. A damage index is a scalar quantity obtained by comparing an understudy spectrum with the baseline spectrum and shows the difference between these spectrums as a result of likely damage. Theoretically, an ideal damage index is a measure which reflects only those spectrum characteristics which are affected directly by the damage, neglecting all other changes resulting from the ambient and working conditions (e.g., expected variations in ambient temperature and vibration).

In recent years, several damage indices have been used by researchers for spectrums comparison and detecting damage. Among those, the following indices are the most common: “root mean square deviation” (RMSD), “mean absolute percentage deviation” (MAPD), “covariance” (COV), and the “correlation coefficient deviation” (CCD) [6]. In this research, CCD was used for damage detection. Equation (2) describes the CCD mathematical relation in terms of the real part of the impedance.

$$\text{Damage Index} = \text{CCD} = 1 - \text{CC} \quad \text{where:}$$

$$\text{CC} = \frac{1}{\sigma_Z \sigma_{Z^0}} \sum_N [\text{Re}(Z_i) - \text{Re}(\bar{Z})] \cdot [\text{Re}(Z_i^0) - \text{Re}(\bar{Z}^0)] \quad (2)$$

Where, Z_i and Z_i^0 are current and baseline value of impedance for i -th frequency, respectively (superscript 0 denotes the baseline or undamaged structural condition), N is the number of measured frequency points, \bar{Z} and \bar{Z}^0 denote mean values, and σ_Z and σ_{Z^0} are standard deviations. The relation produces a scalar quantity, which reflects the differences between the compared spectrums. The most important advantage of this method is that the measurements made by the sensors can be directly used for calculating the damage index.

Previous studies [16], [17] have classified SHM at four levels in terms of their damage-detecting capability and the type of information they collect. The first level and the simplest one is detecting the presence of damage without providing further information about the damage location, the severity, and residual strength of the structure. Level 2 detects the damage location in addition to the presence of it. Level 3 also provides additional information regarding the severity of the damage. Finally, level

4, which is the most complex, costly, and comprehensive level of detection, predicts the residual strength as well as the presence of damage, its location, and severity. However, the above classification has not mentioned about detecting the type of damage in the systems susceptible to different types of damage simultaneously. No doubt, providing a maintenance plan for such systems, requires identifying condition and behavior of each type of damages separately. So, detecting the type of damage and its criticality may be highly valuable.

Numerous researchers have so far used health monitoring techniques to monitor crack and debonding propagation separately. Lalande *et al.* [18] studied impedance at high frequencies for SHM applications in complex structures. They used their proposed method for monitoring the condition of a gear and investigated the variations of the damage index with the presence of a crack. Quattrone *et al.* [19] reported the use of the EMI method to monitor the starting phase of crack propagation during the static testing of a masonry wall reinforced with composite. They showed that EMI technique might detect the existing initial cracks much quicker than the visual techniques. Zagrai and Giurgiutiu [20], [21] also examined the use of the EMI method to monitor cracks in a metallic plate. They extracted relations for electromechanical admittance and empirically reported the success of the implemented method for crack propagation monitoring. Hoshyarmanesh and Abbasi [22] implemented piezo films and the EMI method to detect cracked blades in a prototype turbomachine. Hoon *et al.* [23] and Cavalini *et al.* [24] also reported the capability of the EMI method in the monitoring of crack propagation.

Chung *et al.* [25] studied the bonding quality of a composite patch to a damaged metallic structure using the EMI method. They put the sample under fatigue loading and studied the debonding propagation between the patch and the metallic workpiece. They reported that the occurrence of debonding causes a change in the impedance spectrum. Xu and Liu [26] presented a relation for electromechanical admittance of a piezoelectric patch to model debonding in a composite patch. Bois and Hochard [27] showed the sensitivity of the EMI method to the presence of damage in some layers and also modeled the EMI for interlayer debonding in a multilayer composite. Zhu *et al.* [28] studied the feasibility of locating debonding in a metallic structure repaired by a composite patch and used two different damage index, RMSD and MAPD, for this purpose.

Despite the conducted studies on monitoring crack propagation in metallic structures and debonding in composites, no research has been so far reported the simultaneous monitoring of these two types of damage in a metallic specimen repaired by composite patches. This study aims to investigate the feasibility of simultaneous monitoring of these two types of damage (in terms of crack and debonding propagation) in a specimen and determine which damage occurred at any steps of total damage

propagation. To this goal, using two piezoelectric sensors has been suggested, one mounted on the metal (called metal sensor in this research), and the other mounted on the composite patch (called composite sensor). It is expected that propagation of two different types of damage, such as crack and debonding have different effects on the spectrums provided by the sensors and such a difference may be possibly used to determine which damage is propagating.

2 Samples and Test Procedure

In order to conduct a feasibility study of EMI-based simultaneous monitoring of crack and debonding propagation, a cracked metallic sample repaired by a composite patch was prepared. The sample was an aluminum (AL-2024) specimen with dimensions of $300 \times 100 \times 2 \text{ mm}^3$, which repaired by an $80 \times 80 \times 2 \text{ mm}^3$ glass/epoxy composite patch, shown in Figure 2 schematically. The composite patch was attached to the metal with an epoxy-based adhesive. A miniature milling machine and a scraper knife were used to produce a crack in the metallic component and debonding, respectively.

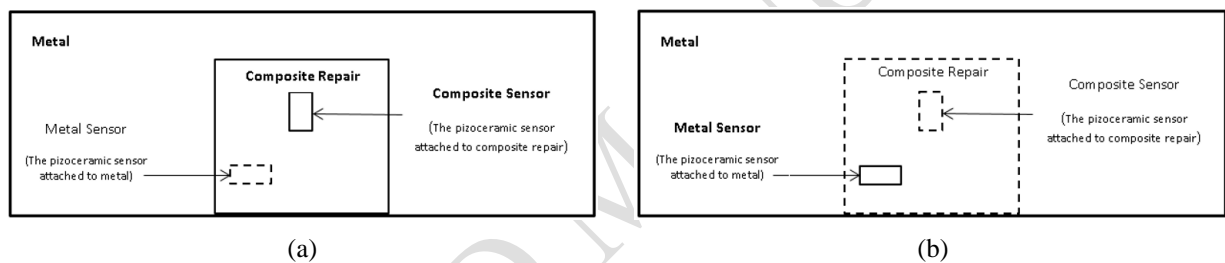


Figure 2. The schematic of the test sample. (a) Top view. (b) Back view

The crack and debonding damage were accumulatively made in the sample. After each step of damage propagation, the measurements provided by the sensors were collected to study the electrical impedance spectrum variations for that particular step. The damage state was indicated as $D_m C_n$ where D and C represent debonding and cracking, respectively. Also, m and n are integers showing the level of damage size caused by debonding and cracking, respectively, as shown in Figure 3. At each step of crack propagation, the crack propagated by 5 mm; and, at each debonding step, the debonding propagated by 20% (relative to the total bonding area). For example, a damage level of $D_2 C_1$ means that the composite patch has been debonded by 40% of the total patch area, and a 5 mm crack exists in the metal specimen.

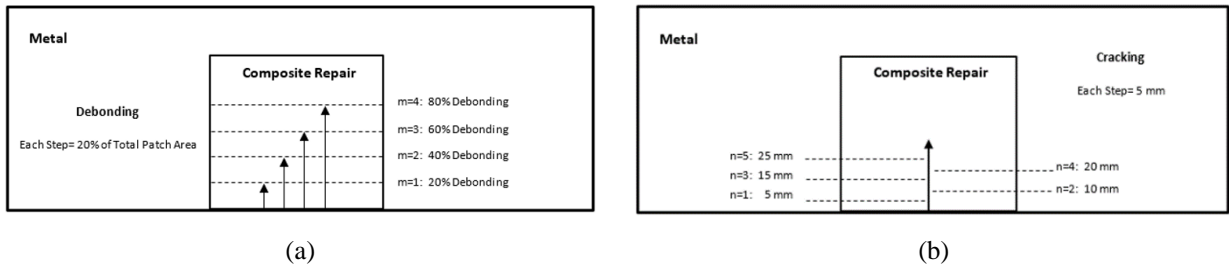


Figure 3. Schematic of damage propagation steps. (a) Debonding propagation steps. (b) Cracking propagation steps

The previous conducted empirical studies on cracked components repaired by composite patches showed that the propagation of damage caused by cracking and debonding of the composite patch could experience different scenarios based on the repair quality. Damage propagation can take the following forms: crack propagation without any debonding; debonding without any crack propagation; and a combination of these two cases [29]–[32]. Therefore, five various damage scenarios were designed to cover the different cases of damage, concisely illustrated in Figure 4.

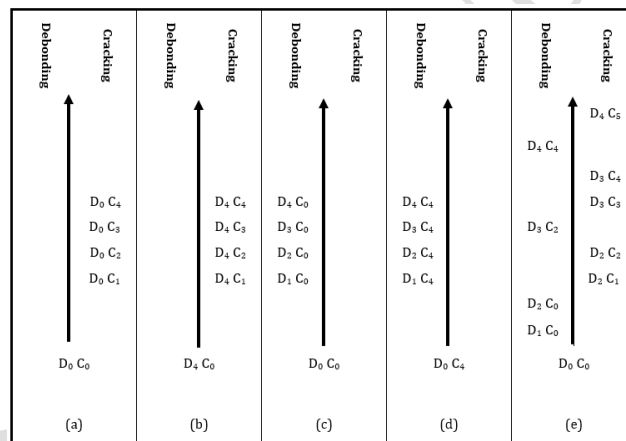


Figure 4. Damage propagation scenarios: (a) Scenario A, (b) Scenario B, (c) Scenario C, (d) Scenario D, and (e) Scenario E.

According to Figure 4, scenario A describes crack propagation without any debonding. Simulating this scenario was achieved manually in four 5mm crack propagation steps. In scenario B, crack propagation started after a significant debonding. First, about 80% of the patch area was debonded, and then the crack was propagated as same as scenario A. In scenario C, debonding propagation occurred without any crack. An overall 80% (relative to the patch area) debonding was propagated manually in four 20% steps. In scenario D, the propagation of debonding in the presence of a crack has been studied. To simulate this scenario, a 20 mm crack was initially produced in the sample, and then, the debonding propagation was done in four 20% steps until an overall 80% propagation. Finally,

scenario *E* was accomplished to model a random crack-debonding propagation in such order that shown in Figure 4-e.

3 Experimental Setup

Two piezoceramics PZT-5H with dimensions of $0.4 \times 9.8 \times 19.6 \text{ mm}^3$ were used to provide simultaneous monitoring. These piezoceramics were attached to the metal and the composite patch, as shown in Figure 5. An impedance evaluation board (Eval-AD5933) manufactured by Analog Devices, Inc, which can measure the electrical impedance up to 100 kHz was implemented. Figure 6 shows the device and its related user interface.



Figure 5. (a) Top view: Sensor attached to the composite patch; (b) Back view: Sensor attached to the metal and crack propagation path

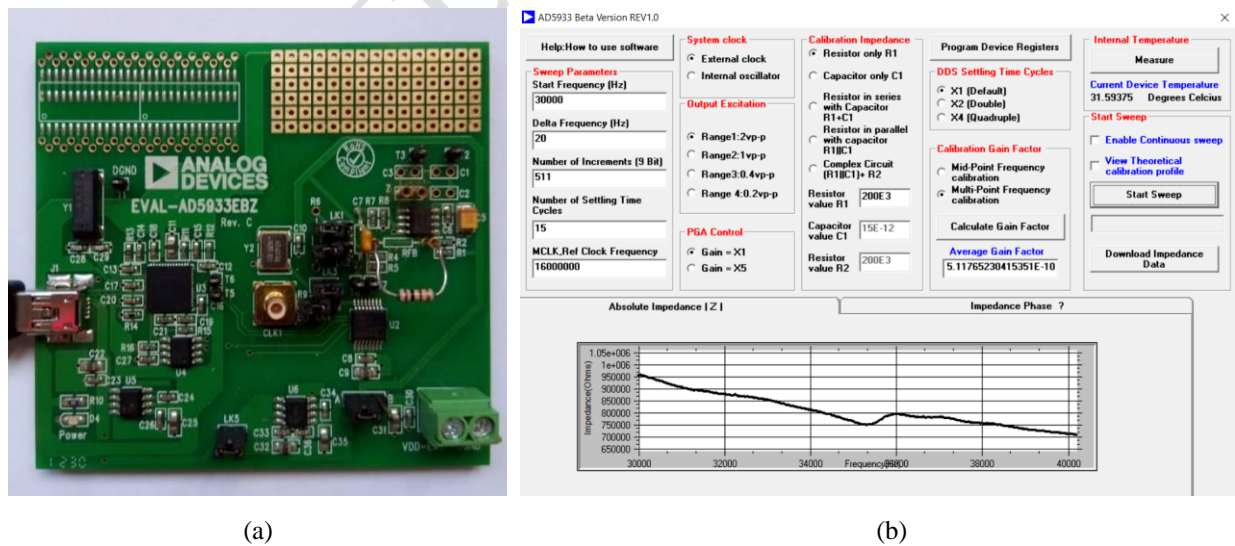


Figure 6. (a) EVAL-AD5933 board manufactured by Analog Devices Inc; (b) The computer user interface of EVAL-AD5933

4 Results and Discussion

According to previous studies, the real parts of impedance and admittance demonstrate higher sensitivity to damage as compared with the imaginary parts [8], [33]. For this reason, the real part of impedance spectrums was analyzed in this study. Figure 7 illustrates how the real part spectrum of the electromechanical impedance changed due to one-step debonding and crack propagation in scenario E for both sensors. As can be seen, the presence of any damage affects the real part of the EMI. However, the Changes in the impedance spectrum in debonding and crack propagation steps are different. In both sensors, crack propagation mostly shifted the spectrum vertically and changed the size of peaks, but the overall shape of the spectrum remained with no significant change. On the other hand, debonding propagation introduced new peaks in the impedance spectrum as well as considerable changes in the overall appearance of the spectrum.

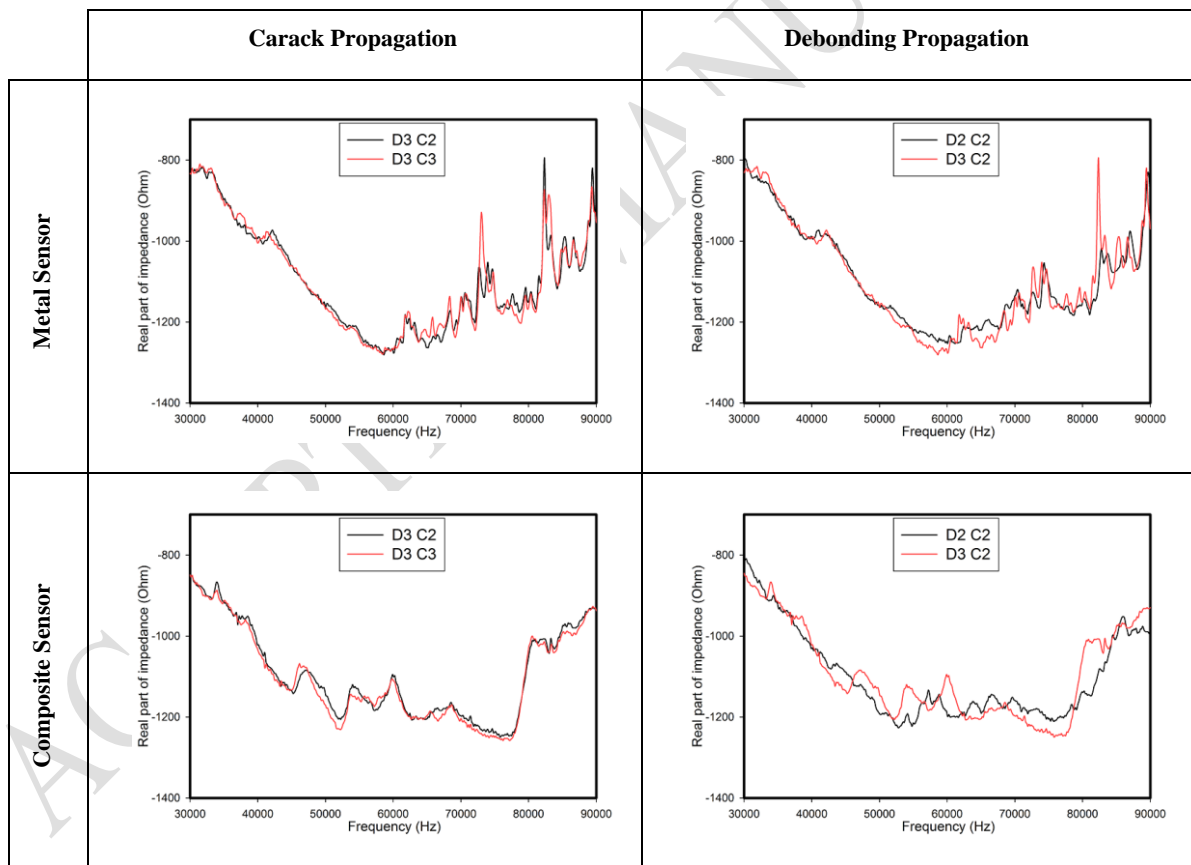


Figure 7. examples of spectrum changing due to different damage type propagation steps for both sensors

The results obtained from calculating the damage index for damage propagation scenarios *A* to *D* are presented in Figure 8. The damage indices for scenarios *A* and *C* were calculated relative to the pristine sample and for scenarios *B* and *D*, the damage indices were calculated relative to D_4C_0 and

D_0C_4 damage states, respectively. Also, Table 1 presents the average of damage indices for scenarios A to D obtained by each sensor.

The results for scenario A (Figure 8-a) and B (Figure 8-b) show that the metal sensor is more sensitive to crack propagation and produces more regular variations in the damage index. As the crack propagated, the damage index for this sensor increased. On the other hand, the damage index chart obtained for the composite sensor remained relatively stable at low values during crack propagation.

In scenario C (Figure 8-c), the damage index for both metal and composite sensors followed an upward trend throughout debonding propagation. However, as can be seen from Table 1, the average value of the composite sensor damage index is five times greater than the metal sensor in this scenario.

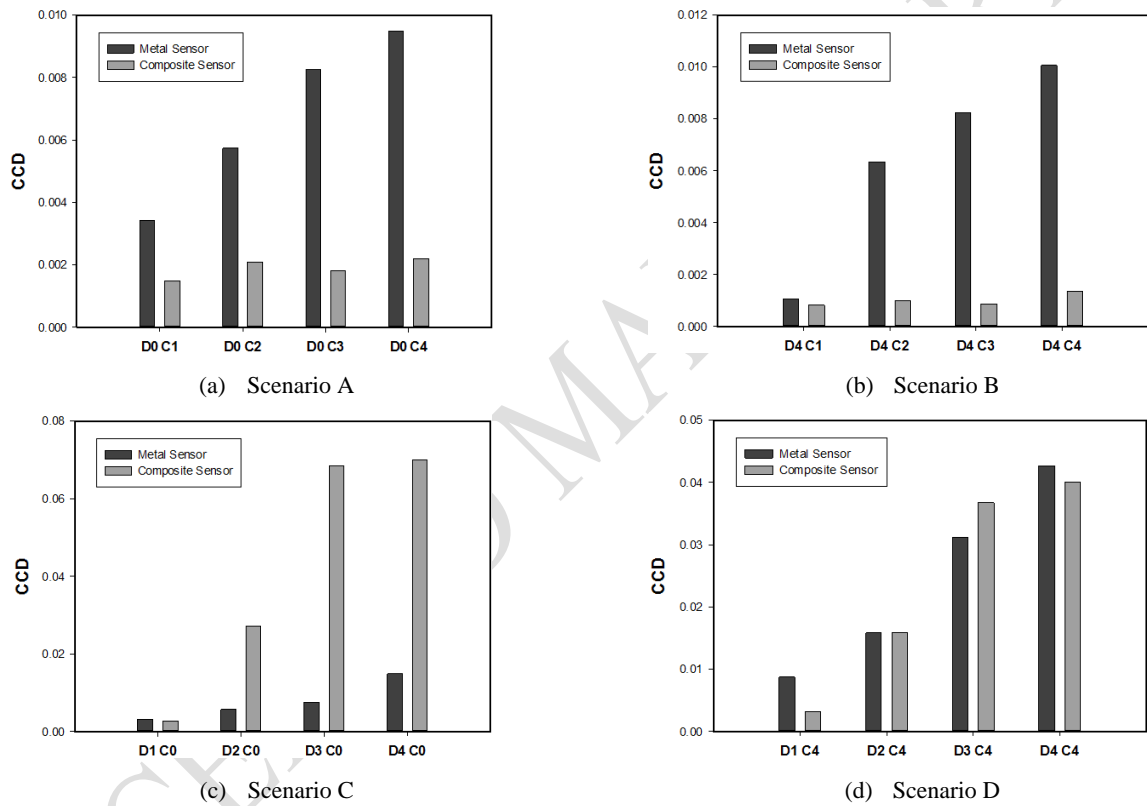


Figure 8. Damage indices for Scenarios (A) to (D)

The damage index charts for the composite and metal sensors in scenario D (Figure 8-d) show that both these sensors are sensitive to the debonding propagation and their indices experienced a dominant upward trend as the debonding area increased. Another critical point according to Table 1 is the damage index values for the metal sensor are obviously higher in scenario D compared to scenario C. It means that the metal sensor capability of debonding detection is more significant in the presence of a crack and as the crack becomes larger the sensibility of this sensor to debonding propagation will increase.

Table 1. Average of damage indices for Scenario (A) to (D)

	Scenario A	Scenario B	Scenario C	Scenario D
Metal sensor	0.00668	0.00657	0.0084	0.02498
Composite sensor	0.00189	0.00118	0.0428	0.02437

Comparison of the results obtained for damage indices of scenarios A to D shows that both metal and composite sensors are sensitive to debonding propagation, and this type of damage increases the damage indices in both these sensors. On the other hand, in crack propagation, only the metal sensor can detect the changes, and the composite sensor does not have acceptable sensibility. Therefore, the following results can be obtained: 1) increase of damage index in the metal sensor associated with negligible variations of the damage index in the composite sensor is indicative of crack propagation, and 2) increase of damage indices in both the metal and composite sensors is indicative of debonding propagation.

The results obtained for scenario E are shown in Figure 9 to check the validity of the previous scenario results. These charts are in good agreement with the abovementioned results. As can be seen, crack propagation did not introduce significant changes in the composite sensor damage index. However, it increases the metal sensor damage index. Conversely, debonding propagation affects both the metal and the composite sensors. These differences can be used in the identification of simultaneous cracking and debonding in the sample.

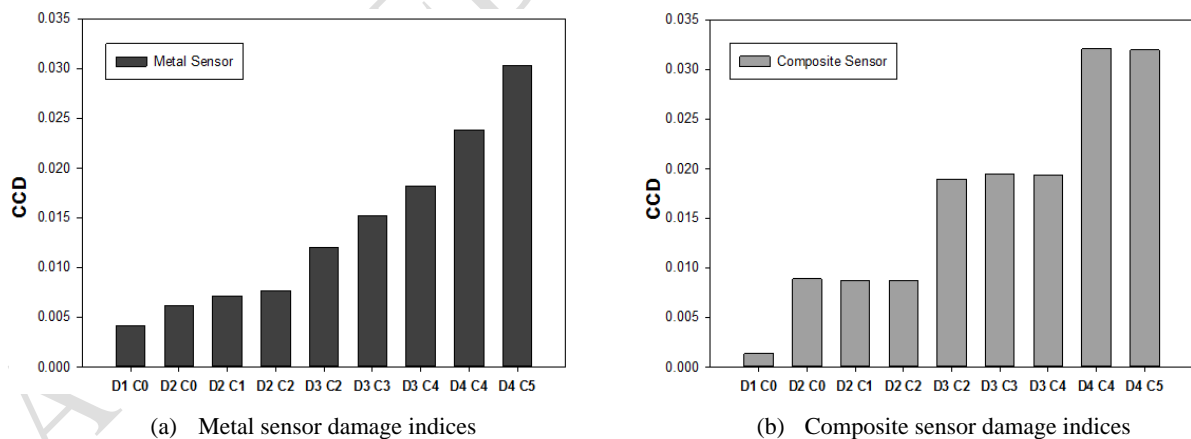


Figure 9. CCD damage indices obtained for Scenario (E)

5 Conclusion

In this study, the ability of the EMI method to identify the damage type among crack and debonding propagation was investigated for a cracked metallic specimen repaired by a composite patch. The EMI

method was selected due to its potential for local monitoring of structures. In order to provide the feasibility of the damage type identification, two piezoelectric sensors were used; one attached to the metallic specimen and the other to the composite patch. As expected, the propagation of crack and debonding produced different variations in the electrical impedance of the sensors, and this difference considered as a basis of the detection process.

Qualitative analysis of EMI real part spectrums demonstrated that growth of any damage types leads to some variation in the electrical impedance spectrum of the sensors, and as compared with crack propagation, the EMI spectrum is more sensitive to debonding propagation. Also, the debonding damage introduces new peaks in the spectrum and changes the overall shape; however crack propagation usually only shifts the spectrum vertically changes the size of some peaks.

Damage Index analysis showed that crack propagation does not significantly change the damage index obtained for the composite sensor; on the other hand, debonding propagation affects both the sensors. In addition, the Metal sensor is more sensitive to debonding propagation in the presence of a crack, and its sensitivity increases as the crack become larger. As a general rule, Increase in the value of metal sensor damage index while the composite sensor damage index experiences negligible change is indicative of crack propagation within the sample. In contrast, a simultaneous increase of metal and composite damage indices is an indication of ongoing debonding propagation inside the sample.

Acknowledgement

This is a preprint of the Work accepted for publication in *Russian Journal of Nondestructive Testing*, ©, copyright 2019, Springer

References

- [1] F. Ricci, F. Franco, and N. Montefusco, "Bonded composite patch repairs on cracked aluminum plates: theory, modeling and experiments," *Adv. Compos. Mater. Anal. InTech*, pp. 445–464, 2011.
- [2] A. A. Baker, "REPAIR EFFICIENCY IN FATIGUE-CRACKED ALUMINIUM COMPONENTS REINFORCED WITH BORON/EPOXY PATCHES," *Fatigue Fract. Eng. Mater. Struct.*, vol. 16, no. 7, pp. 753–765, 1993.
- [3] C. Boller, F.-K. Chang, and Y. Fujino, *Encyclopedia of structural health monitoring*. John Wiley, 2009.
- [4] C. R. Farrar and K. Worden, "An introduction to structural health monitoring," *Philos. Trans. R. Soc. A Math. Phys. Eng. Sci.*, vol. 365, no. 1851, pp. 303–315, 2007.
- [5] S. W. Doebling, C. R. Farrar, and M. B. Prime, "A summary review of vibration-based damage identification methods," *Shock Vib. Dig.*, vol. 30, no. 2, pp. 91–105, 1998.
- [6] W. Na and J. Baek, "A review of the piezoelectric electromechanical impedance based structural health monitoring technique for engineering structures," *Sensors*, vol. 18, no. 5, p. 1307, 2018.

- [7] G. Park, H. Sohn, C. R. Farrar, and D. J. Inman, "Overview of piezoelectric impedance-based health monitoring and path forward," *Shock Vib. Dig.*, vol. 35, no. 6, pp. 451–464, 2003.
- [8] V. Giurgiutiu, *Structural health monitoring: with piezoelectric wafer active sensors*. Academic Press, 2007.
- [9] C.-K. Soh, Y. Yang, and S. Bhalla, *Smart Materials in Structural Health Monitoring, Control and Biomechanics*. Springer, 2012.
- [10] H. Sohn *et al.*, *A review of structural health monitoring literature: 1996-2001*. Los Alamos National Laboratory Los Alamos, NM, 2004.
- [11] Z. A. Chaudhry, T. Joseph, F. P. Sun, and C. A. Rogers, "Local-area health monitoring of aircraft via piezoelectric actuator/sensor patches," in *Smart Structures & Materials '95*, 1995, pp. 268–276.
- [12] T. Ayres, Z. Chaudhry, and C. Rogers, "Localized health monitoring of civil infrastructure via piezoelectric actuator/sensor patches," in *Proceedings, SPIE's 1996 Symposium on Smart Structures and Integrated Systems*, 1996, vol. 2719, pp. 123–131.
- [13] V. Giurgiutiu and C. A. Rogers, "Electro-mechanical (E/M) impedance method for structural health monitoring and non-destructive evaluation," *Struct. Heal. Monit. Status Perspect.*, pp. 18–20, 1997.
- [14] V. Giurgiutiu and A. N. Zagrai, "Characterization of piezoelectric wafer active sensors," *J. Intell. Mater. Syst. Struct.*, vol. 11, no. 12, pp. 959–976, 2000.
- [15] V. Giurgiutiu, A. Zagrai, and J. J. Bao, "Piezoelectric wafer embedded active sensors for aging aircraft structural health monitoring," *Struct. Heal. Monit.*, vol. 1, no. 1, pp. 41–61, 2002.
- [16] N. N. A. Brigman, "Structural health monitoring in commercial aviation." Massachusetts Institute of Technology, 2012.
- [17] C. R. Farrar and N. A. J. Lieven, "Damage prognosis: the future of structural health monitoring," *Philos. Trans. R. Soc. A Math. Phys. Eng. Sci.*, vol. 365, no. 1851, pp. 623–632, 2007.
- [18] F. Lalonde, C. A. Rogers, B. W. Childs, and Z. A. Chaudhry, "High-frequency impedance analysis for NDE of complex precision parts," in *1996 Symposium on Smart Structures and Materials*, 1996, pp. 237–243.
- [19] R. Quattrone, J. Berman, and J. Kamphaus, "Upgrade and Monitoring of Unreinforced Masonry Structures Using Fiber Reinforced Polymers," *Plast. Build. Constr.*, vol. 22, pp. 9–12, 1998.
- [20] V. Giurgiutiu and A. N. Zagrai, "Electro-mechanical impedance method for crack detection in metallic plates," in *6th Annual International Symposium on NDE for Health Monitoring and Diagnostics*, 2001, pp. 131–142.
- [21] A. N. Zagrai and V. Giurgiutiu, "Electro-mechanical impedance method for crack detection in thin wall structures," in *3rd Int. Workshop of Structural Health Monitoring*, 2001, pp. 12–14.
- [22] H. Hoshyarmanesh and A. Abbasi, "Structural health monitoring of rotary aerospace structures based on electromechanical impedance of integrated piezoelectric transducers," *J. Intell. Mater. Syst. Struct.*, vol. 29, no. 9, pp. 1799–1817, 2018.
- [23] T. Hoon, M. Toshihiko, C. K. Tang, and W. K. Chiu, "Fatigue crack detection using piezoelectric elements," in *Structural Integrity and Fracture International Conference (SIF'04)*, 2004, pp. 137–142.
- [24] A. Ap Cavalini Jr, R. M. F. Neto, and V. Steffen Jr, "Electromechanical Impedance Based Crack Detection for a Rotating Machine," in *Topics in Modal Analysis I, Volume 7*, Springer, 2014, pp. 31–40.
- [25] J. Chung, "Monitoring the integrity of composite patch structural repair via piezoelectric actuators/sensors," 1995.
- [26] Y. G. Xu and G. R. Liu, "A modified electro-mechanical impedance model of piezoelectric actuator-sensors for debonding detection of composite patches," *J. Intell. Mater. Syst. Struct.*, vol. 13, no. 6, pp. 389–396, 2002.
- [27] C. Bois and C. Hochard, "Monitoring of laminated composites delamination based on electro-mechanical impedance measurement," *J. Intell. Mater. Syst. Struct.*, vol. 15, no. 1, pp. 59–67, 2004.
- [28] J. Zhu, Y. Wang, and X. Qing, "A real-time electromechanical impedance-based active monitoring for composite patch bonded repair structure," *Compos. Struct.*, vol. 212, pp. 513–523, 2019.

[29] H. Hosseini-Toudeshky, B. Mohammadi, and S. Bakhshandeh, "Crack trajectory analysis of single-side repaired thin panels in mixed-mode conditions using glass/epoxy patches," *Comput. Struct.*, vol. 86, no. 9, pp. 997–1005, 2008.

[30] H. HOSSEINI-TOUDESHPKY, B. Mohammadi, and S. Bakhshandeh, "Mixed-mode fatigue crack growth of thin aluminium panels with single-side repair using experimental and numerical methods," *Fatigue Fract. Eng. Mater. Struct.*, vol. 30, no. 7, pp. 629–639, 2007.

[31] H. Hosseini-Toudeshky, B. Mohammadi, G. Sadeghi, and H. R. Daghyani, "Numerical and experimental fatigue crack growth analysis in mode-I for repaired aluminum panels using composite material," *Compos. Part A Appl. Sci. Manuf.*, vol. 38, no. 4, pp. 1141–1148, 2007.

[32] H. Hosseini-Toudeshky, S. Bakhshandeh, B. Mohammadi, and H. R. Daghyani, "Experimental investigations on fatigue crack growth of repaired thick aluminium panels in mixed-mode conditions," *Compos. Struct.*, vol. 75, no. 1, pp. 437–443, 2006.

[33] A. N. Zagrai, "Piezoelectric-wafer active sensor electro-mechanical impedance structural health monitoring." University of South Carolina, 2002.

ACCEPTED MANUSCRIPT